REPORT DOCUMENTATION PAGE

Form Approved
OMB No. 0705-0188

1. AGENCY USE ONLY (Leave blank)	2. REPORT DATE	3. REPORT TYPE AND DATES COVERED
	970228	Technical 1 Report, Dec '95-Nov '96

4. TITLE AND SUBTITLE

Synthesis of Ceramics from Solutions: Fuctionally Graded Composites, NanoComposites and Single Crystal Thin Films

5. FUNDING NUMBERS

AFOSR F49620-96-1-0003

6. AUTHOR(S)

Fred F. Lange

7. PERFORMING ORGANIZATION NAME(S) AND ADDRESS(ES)

Materials Department
College of Engineering
University of California
Santa Barbara, CA 93106-5050

9. SPONSORING/MONITORING AGENCY NAME(S) AND ADDRESS(ES)

Dr. Alexander Pechenik
AFOSR/PKA
110 Duncan Avenue, Suite B115
Bolling AFB DC 20332-8080

10. SPONSORING/MONITORING AGENCY REPORT NUMBER

Techical Report No 1

11. SUPPLEMENTARY NOTES

12A. DISTRIBUTION/AVAILABILITY STATEMENT

A

12B. DISTRIBUTION CODE

13. ABSTRACT (Maximum 200 words)

The crystallization, transformation, and partitioning of amorphous PbO-ZrO_2-TiO_2 powders produced by pyrolytic decomposition of mixed alkoxide precursors were investigated. Materials have the general formulation $Pb_{1+\chi}Ti_{[1/(1+\phi)]}Zr_{[\phi/(1+\phi)]}O_{3+\chi}$, where $-0.2 \leq \chi \leq 0.2$ is the fraction PbO excess/deficiency and $0 \leq \phi \leq 1$ is the Zr/Ti molar ratio. Most compositions first crystallized as a metastable fluorite structure with varying degrees of pyrochlore-like cation ordering, which transformed to a single perovskite phase upon additional heat treatment. Higher Zr/Ti ratios enhanced the retention of fluorite and reduced the incidence of cation ordering. Compositions with off-stoichiometric amounts of PbO often yielded extended solid solutions prior to partitioning. For example, metastable perovskites with as much as 20% PbO deficiency ($\chi = -0.2$) could be prepared for $0 \leq \phi \leq 1$, but only ~10% PbO excess could be incorporated in solution for $0.33 \leq \phi \leq 1$. Increasing PbO content was found to promote crystallization, suggesting that this oxide acts as a network modifier enhancing mobility within the initial amorphous precursor powder. Higher PbO was also noted to favor cation ordering in the metastable phase and to accelerate the transformation to perovskite, as well as to promote partitioning for hyperstoichiometric compositions. The findings are discussed in light of structural relationships between the fluorite, pyrochlore and perovskite phases, as well as current understanding of the thermodynamics of the system.

14. SUBJECT TERMS	15. NUMBER OF PAGES
crystallization, transformation, partitioning , PbO, ZrO_2, TiO_2, PZT, Metastable Phase	33
	16. PRICE CODE

17. SECURITY CLASSIFICATION OF REPORT	18. SECURITY CLASSIFICATION OF THIS PAGE	19. SECURITY CLASSIFICATION OF ABSTRACT	20. LIMITATION OF ABSTRACT
Unclassified	Unclassified	Unclassified	

Synthesis of Ceramics From Solutions: Functionally Graded Composites, NanoComposites and Single Crystal Thin Films

Contract AFOSR F49620-96-1-0003

period: December 1995- November 1996

February 1997

From

Materials Department
College of Engineering
University of California
Santa Barbara, CA 93106

Technical Report 1

METASTABILITY OF THE FLUORITE, PYROCHLORE, AND PEROVSKITE STRUCTURES IN THE PbO-ZrO_2-TiO_2 SYSTEM

Andrew D. Polli, Fred F. Lange, and Carlos G. Levi

Submitted to the J. American Ceramic Society

METASTABILITY OF THE FLUORITE, PYROCHLORE, AND PEROVSKITE STRUCTURES IN THE PbO-ZrO_2-TiO_2 SYSTEM

Andrew D. Polli, Fred F. Lange, and Carlos G. Levi

Materials Research Laboratory and Materials Department
University of California, Santa Barbara, CA 93106-5050

ABSTRACT

The crystallization, transformation, and partitioning of amorphous PbO-ZrO_2-TiO_2 powders produced by pyrolytic decomposition of mixed alkoxide precursors were investigated. Materials have the general formulation $Pb_{1+\chi}Ti_{[1/(1+\phi)]}Zr_{[\phi/(1+\phi)]}O_{3+\chi}$, where $-0.2 \leq \chi \leq 0.2$ is the fraction PbO excess/deficiency and $0 \leq \phi \leq 1$ is the Zr/Ti molar ratio. Most compositions first crystallized as a metastable fluorite structure with varying degrees of pyrochlore-like cation ordering, which transformed to a single perovskite phase upon additional heat treatment. Higher Zr/Ti ratios enhanced the retention of fluorite and reduced the incidence of cation ordering. Composition with off-stoichiometric amounts of PbO often yielded extended solid solutions prior to partitioning. For example, metastable perovskites with as much as 20% PbO deficiency ($\chi = -0.2$) could be prepared for $0 \leq \phi \leq 1$, but only ~10% PbO excess could be incorporated in solution for $0.33 \leq \phi \leq 1$. Increasing PbO content was found to promote crystallization, suggesting that this oxide acts as a network modifier enhancing mobility within the initial amorphous precursor powder. Higher PbO was also noted to favor cation ordering in the metastable phase and to accelerate the transformation to perovskite, as well as to promote partitioning for hyperstoichiometric compositions. The findings are discussed in light of structural relationships between the fluorite, pyrochlore and perovskite phases, as well as current understanding of the thermodynamics of the system.

I. INTRODUCTION

The development of thin ferroelectric oxide films has recently been at the center of much research. Such films are commonly prepared through solution routes, like sol-gel [1-5] or metal-organic deposition (MOD), [6,7] which usually require a subsequent heat treatment in order to pyrolyze the organic material and crystallize the film into the desired inorganic. [8] Crystallization in these processes occurs at relatively low homologous temperatures ($T/T_M < 0.5$), where the driving force is quite large but the mobility is only marginal, i.e. sufficiently high to enable the short range rearrangements necessary for crystal formation, but not the long range redistribution of species. [9] As such, the first product of crystallization typically has nanoscale grains and often exhibits extended solid solubility and/or metastable crystal structures. For example, Balmer et al. [10] showed that single phase tetragonal (T) or (cubic) fluorite (F) $Zr_{1-x}Mg_xO_{2-x}$ solid solutions with up to 20 mole%MgO could be produced from an amorphous precursor powder through crystallization in the monoclinic (M) ZrO_2 + MgO phase field. Higher solubility extensions, up to ~40 mole%, have been reported in ZrO_2-Al_2O_3 [11] and ZrO_2-Fe_2O_3, [12] whereas Jayaram et al. [13] showed that the fluorite field could be extended across the entire composition range in ZrO_2-Y_2O_3.

It has been reported that precursor-derived compositions along the $PbTiO_3$-$PbZrO_3$ (PZT) quasibinary in the PbO-ZrO_2-TiO_2 ternary, Figure 1, crystallize to a fine-grained metastable fluorite [14-16] or pyrochlore [17] phase prior to formation of the equilibrium perovskite structure. Further, it has been noted that the selection of such transitional phases promotes the trapping of porosity during the solid state epitaxy of single crystal films from fine-grained metastable PZT layers. [16] The problem was ascribed to the additional free energy available to drive the single crystal/polycrystal interface when epitaxial growth involves a phase transformation.

The present investigation was undertaken to further our understanding of the origin of metastable structures in this important family of ferroelectric materials, as well as the roles of ZrO_2 and PbO in the phase selection process. Powders were selected for this study, in preference to films, to obviate any potential influence of the substrate. Moreover, powder specimens are also simpler to process and afford larger diffraction volumes than films, which facilitate the analysis. Previous experience[18] had shown, however, that the synthesis of homogeneous, amorphous PZT powders suitable to study the crystallization sequence is not a trivial matter, since Pb tends to volatilise [18] due to the low oxygen partial pressure that is locally present during the decomposition of metal-organic precursor containing Pb. Procedures established in the cited study to avoid this problem were followed [18] in the present work.

II. EXPERIMENTAL PROCEDURES

(1) Synthesis of PZT Powders

Lead zirconate and titanate alkoxide solutions were prepared using lead(II) acetate trihydrate, zirconium(IV) butoxide, and titanium(IV) isopropoxide. Processing of each solution started with the dehydration of the Pb acetate in a three neck flask by holding the acetate powder at 110°C for 30 min under vacuum. The flask was then backfilled with N_2 and moved to a drybox, where solvent and alkoxide were sequentially added. Either ethanol or n-propanol were used as the solvent. Different solutions, one set containing Pb and Ti precursors, and another set containing Pb and Zr precusors were prepared with an alkoxide-to-solvent concentration of 0.85mol/l; each set of solutions has a specific Pb/Ti (or Pb/Zr) ratio. The dehydrated Pb acetate was insoluble at room temperature so the flask was removed from the drybox for dissolution and the two solutions were refluxed at

~85°C under a N_2 pressure for 12-30 hr. Each Pb/Ti solution was assayed for its oxide content and mixed with its complimary Pb/Zr solution to prepare precursor solutions with Zr/Ti molar ratios of 0/100, 25/75, and 50/50 and PbO deviations from stoichiometry of ±20%, ±10%, -15% and +5% relative to $Pb(Zr,Ti)O_3$.

Powders were prepared by direct hydrolysis of the alkoxide solutions by rapid mixing of an equal volume of de-ionized water. Hydrolysis produced precipitate that was dried at 100°C, ground, and pyrolyzed in air at 300°C for 2 h. As demonstrated elsewhere,[18] his procedure yielded an amorphous oxide powder, nearly free from carbon. The pre-pyrolyzed powders were then heat treated by placing them in a container and rapidly inserting them into a tube furnace that had been pre-heated to the desired temperature (400-1000°C). Pt crucibles were used for treatments below 800°C and Al_2O_3 boats for higher temperatures. After a typical treatment period of 5 min to 1 h, the powder was pushed out of the furnace and cooled in air. All heat treatments were performed in an oxygen atmosphere with a continuous flow of O_2 through the furnace tube.

(2) Microstructure Characterization.

Identification of crystalline phases was accomplished by X-ray diffraction (XRD), aided when necessary by selected-area electron diffraction (SAD). Most XRD patterns were collected in the 2θ range of 10° to 70° at 0.75°/min. A Ni sample holder provided several Ni diffraction peaks for calibration. Lattice parameters were determined for the perovskite phase from profiles collected between $20 \leq 2\theta \leq 95°$ at 0.15°/min. with an internal Cu_2O standard. These patterns resulted in 13-18 strong diffraction peaks for fitting with Pearson VII curves. A least-squares lattice parameter refinement was performed after asigning each measured d-spacings to a particular set of crystallographic planes.

Transmission electron microscopy (TEM) samples were prepared by first grinding a small amount of the powder with a mortar and pestle. Isopropanol was added and the powder ground again, creating a suspension of fine particles. This suspension was poured into a vial, stirred ultrasonically for 30 min, and allowed to settle for an additional 30 min to separate the coarser particles. A few drops of the suspension were then applied to a 3 mm, 200 mesh copper grid holding a carbon-coated formvar film, and allowed to dry over a lamp for several minutes. Many of the particles on the film were sufficiently thin to allow electron transmission and thus diffraction analysis in the TEM.

III. RESULTS

The range of compositions investigated is denoted by the shaded area in Figure 1(a), bounded by $0 \leq Zr/Ti \leq 1$ and PbO contents from 44.4 mole% (20% deficiency) to 54.5 mole% (20% excess). The general composition can be conveniently expressed as $Pb_{1+\chi}Ti_{[1/(1+\phi)]}Zr_{[\phi/(1+\phi)]}O_{3+\chi}$, where χ is the fraction PbO excess/deficiency and ϕ is the Zr/Ti molar ratio. The onset of crystallization, phase selection, and partitioning behavior of the powders was found to change significantly with both χ and ϕ. The more notable findings were:

- Partitionless crystallization is more readily observed in compositions with PbO deficiency than in those with PbO excess.
- The first product of crystallization is often a metastable fluorite structure (F) which may exhibit a slight degree of pyrochlore-like cation ordering.
- Single phase perovskites (P) with extended solubility were synthesized on both sides of the PZT field, but appear to be less stable for $\chi > 0$.
- Partitioning leads to the precipitation of equilibrium PbO on the hyperstoichiometric ($\chi > 0$) perovskite side whereas some hypostoichiometric titanate compositions ($\phi = 0, \chi < 0$) precipitate a metastable $PbTi_3O_7$ phase.

These findings are detailed in the following sections.

(1) Crystallization and Phase Selection.

The results for the 5 min isothermal treatments on the pre-pyrolyzed powders are summarized in Figure 1(b). All compositions showed no evidence of crystallinity following the 300°C pyrolysis treatment with either XRD or electron SAD, and remained amorphous after subsequent rapid heating and isothermal treatment for 5 min at 400°C. In general, stoichiometric compositions and those with excess PbO ($\chi \geq 0$) were found to crystallize at lower temperatures than those deficient in PbO ($\chi < 0$), independent of Zr/Ti ratio. For example, Figure 1(b) shows that compositions with $\chi \geq 0$ had either initiated or completed crystallization after 5 min at 500°C, whereas those with $\chi < 0$ were still amorphous after the same treatment. Powders with $\phi = 1$ and $\chi = 0.2$ remained gray following the 300°C pyrolysis, suggesting the presence of a substantial amount of free carbon; these same compositions formed elemental Pb after treating for 5 min at 500°C, similar to other carbon-rich precursor-derived materials. [18] Crystallization of these powders without PbO reduction could not be achieved under any of the conditions investigated and hence it is not discussed further in this paper.

The most general sequence of events observed upon heat treatment of most compositions included the crystallizition of a single, metastable phase, its transformation to a the perovskite structure and the partioning of second phases. The transitional metastable phase had the fluorite structure, in agreement with previous reports, [14-16] but exhibited some evidence of cation ordering in a pyrochlore-like pattern, as noted below. A typical SAD pattern for the transitional metastable phase is shown in Figure 2(a), with that of perovskite is shown for comparison in Figure 2(b).

The reflections due to apparent cation ordering are either quite weak or absent. They were undetectable in the XRD spectra and even in the best SAD patterns they were only discernible in the negative but difficult to capture in print, and thus could be printed here. Rotationally averaged intensity profiles from digitized images of the SAD negatives do show evidence of small "bumps" where the cation ordering peaks associated with the pyrochlore structure are expected, as illustrated in Figure 2(c). The strongest evidence of pyrochlore phase found in SAD patterens occured for the two compositons with $\phi = 1$, $\chi = 0.1$ and $\phi = 0.33$, $\chi = -0.2$, corresponding to the top and bottom curves of Fig. 2c, both of which could be fully crystallized without the evidence of the perovskite structure.* All the strong reflections in the SAD patterns for these materials could be indexed to a fluorite structure. The weak reflection next to the $(200)_F$ peak in Figure 2(c) was indexed to the (331) plane of a pyrochlore cell with twice the lattice parameter of the parent fluorite. An additional, even weaker, reflection corresponding to the (511) pyrochlore peak is also noted in Figure 2(c) for the $\phi = 0.33$, $\chi = -0.2$ material. The intensity of the weak (331) ring decreased with increasing ZrO_2 content for the $\chi = -0.2$ materials, becoming undetectable at $\phi = 1$, as noted by the middle curve in Figure 2(c). But, when the PbO was increased to $\chi = 0.1$, the (331) ordering reflection reappeared for the latter Zr/Ti ratio as shown in upper curve in Figure 2(c). Since the ordering reflections are never fully developed and a distinct pyrochlore phase does not evolve prior to the emergence of perovskite, the intermediate, metastable phase is perhaps most appropriately described as a fluorite with a slight degree of pyrochlore-like cation ordering (see Discussion below).

---

* The $\phi = 0.33$, $\chi = -0.1$ material, shown in Figure 1(b) as containing a mixture of fluorite and perovskite after 5 min at 600°C, was also found to form only fluorite when processed at 550°C.

The stability of the metastable fluorite is clearly a function of ZrO_2 content. For the compositions leanest in PbO (χ = -0.2) fully crystallized fluorite without a trace of perovskite was obtained for the ϕ = 1 and ϕ = 0.33 after 5 min at 600°C as shown in Figure 1(b). Conversely, the titanate (ϕ = 0) with the same PbO deficiency contained some perovskite after the same treatment, and transformed to single phase perovskite at either higher temperatures or longer times, consistent with the metastable nature of the metastable fluorite form. Increasing the PbO content led to the emergence of perovskite at higher ZrO_2 contents ($\phi > 0$) under the same processing conditions, as noted in Figure 1(b). As the PbO content became hyperstoichiometric ($\chi > 0$), single phase fluorite was not observable for any composition with ϕ = 0 or 0.33 under the conditions of this figure, but was still obtained for the composition ϕ = 1, χ = 0.1. The absence of fluorite for compositions with the lower ZrO_2 contents and $\chi \geq 0$ in Figure 1(b) suggests that pervoskite formation may have occurred directly from the amorphous phase. This is further supported by the observation that, for short treatments at ~500°C, the perovskite was found mixed with residual amorphous phase without detectable evidence of the metastable fluorite in XRD. (One should note, however, that TEM examination was not sufficiently extensive to rule out conclusively the presence of fluorite.) Conversely, work by other investigators has shown that fluorite does precede the evolution of perovskite for the Ti-rich compositions when crystallization is effected at lower temperatures and longer times, e.g. 400°C/1h. [16]

The hyperstoichiometric titanates (ϕ = 0, $\chi \geq 0.05$) were all found to contain two-phases of different composition even after 5 min at 500°C as shown in Figure 1(b). Neither the transitional fluorite phase nor perovskite could be produced free from PbO for these compositions, suggesting again, that if intermediate single phases had evolved during crystallization their stability was so marginal that they rapidly evolved into the equilibrium assemblage at the temperatures investigated.

(2) Extended Solubility

All compositions forming single phase fluorite in the range investigated clearly represent very large extensions in solubility relative to the equilibrium ZrO_2 phase field in Figure 1(a). The lattice parameters for these metastable solutions are given in Table 1. The effect of ZrO_2 and PbO on the lattice parameter is illustrated by the shift in d-spacings in Figure 2(c). For those configurations in which the fluorite was found mixed with perovskite after a short crystallization treatment, the former appeared to exhibit no change in lattice parameter as the transformation proceeded, indicating again that the initial fluorite phase was supersaturated and transformed to perovskite without partitioning.

Perhaps a more important observation from a technological perspective is that the perovskite structures with extended solubility were synthesized in the composition range investigated. It has been reported[19] that the equilibrium homogeneity range of the (cubic) perovskite phase field at 1100°C extends in the PbO deficient direction down to $\chi \approx -0.1$, -0.037 and -0.025 for $\phi = 0$, 0.33 and 1, respectively. (There is no indication, however, that the finite homogeneity range for PZT has been recognized in either of the reported binaries, [20,21] or in other studies on the ternary. [22]) The equilibrium solubility is anticipated to be lower at the temperatures investigated and thus all the single phase perovskites observed for $\chi \neq 0$ in Figure 1(b) are extended solid solutions. All data points in this figure identified as single phase, off-stoichiometric perovskites were confirmed by SAD, e.g. Figure 2(b), which revealed no detectable fluorite/pyrochlore residue, nor precipitation of a second phase under the treatments specified.

The refined lattice parameters of the equilibrium and metastable perovskites are reported in Table 1. The cubic form, which is stable at the processing temperatures, readily transforms to tetragonal upon cooling. The tetragonality (c/a

ratio) of the structure decreases with increasing Zr content (ϕ), and with decreasing PbO content, as illustrated in Figures 3(a) and 4. Conversely, the unit cell volume increases with higher Zr contents, as noted in Figure 3(b), but the effect of PbO is not as well behaved. Figure 3(b) also compares the volume per formula unit in the perovskite and fluorite structures (one unit cell in the former and half a unit cell in the latter), revealing that the transformation involves a contraction in volume of ~9%. This is a significant volume change which may translate into either porosity or residual stresses in a precursor-derived film.

(3) Partitioning Behavior.

The supersaturated perovskites can have significant stability against partitioning, particularly for the PbO deficient compositions. In fact, perovskites with χ = -0.1 and ϕ = 0.33 and 1 failed to partition during 5 min heat treatments at temperatures as high as 1000°C, whereas, as shown in Figure 1(b), those with χ = 0.1 and the same Zr/Ti ratio precipitated PbO at ~800°C. The stability of these hyperstoichiometric perovskites appears to increase with ZrO_2 content. For example, the ϕ = 1, χ = 0.1 composition in Figure 5 could be held for 4 h at 600°C without partitioning, whereas as shown in Figure 6, a composition with the same PbO content and ϕ = 0.33 appeared to initiate precipitation after 5 min at 700°C. Note, however, that partitioning at 700°C is still relatively sluggish, and PbO precipitation is far from complete even after 2 h, cf. profiles (d) and (e) in Figure 6. Conversely as shown in Figure 1(b), the titanate (ϕ = 0) compositions with excess lead partitioned in 5 min at temperatures as low as 500°C, while those deficient in PbO initiated partitioning only at ~1000°C for equivalent times, as illustrated by spectrum (d) in Figure 4.

Partitioning on the hyperstoichiometric ($\chi > 0$) side of the PZT field consistently led to precipitation of PbO, as expected from the phase diagram in

Figure 1(a). Decomposition of the hypostoichiometric ($\chi < 0$) perovskites however, could take place along different paths. The binary materials ($\phi = 0$) with PbO deficiency precipitated a titanium-rich lead titanate, $PbTi_3O_7$, instead of the equilibrium rutile (or a metastable anatase) phase as shown in Figure 4. The ternaries with the same PbO deficiency formed fluorite + perovskite combinations but with some differences. The $\phi = 0.33$, $\chi = -0.2$ material initiated the F $\rightarrow$ P transformation in a partitionless manner, but partitioning ensued in the later stages, before a single phase perovskite could be produced. As partitioning occurred, the lattice parameter of the metastable fluorite started to change toward that of the equilibrium ZrO_2-rich phase. It was noted, however, that the second phase was still fluorite (cubic) and not monoclinic or tetragonal zirconia,[†] both of which are more stable at all relevant temperatures near the ZrO_2 rich corner of the ternary. The $\phi = 1$, $\chi = -0.2$ material was also very sluggish to form perovskite from the transitional fluorite phase but the transformation was still partitionless, as indicated by the invariance of the fluorite lattice parameter during the process. Moreover, there was no evidence of peak-splitting in the XRD pattern of perovskite, as would be expected from Figure 3(a) if its PbO content were increasing toward equilibrium.

IV. DISCUSSION

A number of issues emerge from the results of the present experiments and similar studies by other authors. A rationale for the evolution of metastable fluorite and pyrochlore in stoichiometric PZT is presented first, followed by a discussion of

---

[†] Work in other systems has shown that the tetragonal and cubic phases may be confused when the solute content in the former drives the c/a ratio toward unity.[94BLL] While no evidence of tetragonal was evident in the XRD or SAD patterns, it cannot be conclusively ruled out that the ZrO_2 rich phase may be slightly tetragonal. The difference, however, is not critical for this discussion.

the effects of chemical composition on the crystallization behavior and phase selection processes.

(1) Selection of Metastable Fluorite

Drawing an analogy to the selection of metastable fluorite (C1) over the equilibrium ($D5_3$) form of pure Y_2O_3, [13] Seifert et al. [16] suggested that the perovskite structure could be similarly suppressed in favor of fluorite because neither the anions or cations needed to be ordered during crystallization. The argument was further elaborated by Levi, [9] who noted the structural relationship between the perovskite and fluorite structures. The elements of this relationship are illustrated in Figures 7(a) and (b), which show the arrangement of cations and anions on successive (00ℓ) planes. The cations in perovskite are typically described as forming a b.c.c.-type array, but may also be represented by a *face-centered tetragonal* lattice with A^{2+} and B^{4+} alternating in successive $(002)_P$ plane as shown in Figure 7(a). (The lattice parameters of this structure would be $a = \sqrt{2}\,a_P$ and $c = a_P$.) Conversely, the cations in fluorite are in a *face-centered cubic* array, wherein all positions are equivalent, but could also be described as forming a body-centered tetragonal lattice with parameters $a = a_F/\sqrt{2}$ and $c = a_F$. The A^{2+} and B^{4+} cations in perovskite are coordinated by 12 and 6 anions, respectively, whereas all cations in a defect fluorite with stoichiometry M_2O_3 would be coordinated by 6 anions as noted by Jayaram et al. [13] Comparison of the anion arrangements in both structures further shows that the oxygen pattern in the 1/2 layer of perovskite is essentially identical to that in the 1/4 and 3/4 layers of the fluorite unit cell (represented in Figure 7 without the small displacements associated with the presence of anion vacancies).

Crystallization of perovskite under strong diffusional constraints is likely to induce disorder, manifested as cation mixing between the A and B lattices. While A^{2+} could be reasonably accomodated in an octahedral (B) site, placing the smaller

B^{4+} cations in 12-fold coordinated sites would be clearly much less favorable. In contrast, all cation sites in the defect fluorite are 6-fold coordinated and thus compatible in principle with both A^{2+} and B^{4+}. From this perspective the fluorite structure offers not only a kinetic advantage over perovskite, since cation ordering is not required for crystallization, but may also be *energetically favored* over a hypothetical perovskite with fully disordered cations.

(2) The Transitional Pyrochlore-like Ordering

The structural relationships between fluorite and pyrochlore have been described by Longo et al. [23] and Subramanian et al. [24] In essence, both structures exhibit an f.c.c. cation arrangement, but the A and B cations in the pyrochlore structure are ordered in alternating rows along ⟨110⟩ directions, as depicted in Figure 7(c), with rows rotated by 90° in consecutive cation planes normal to the [001] direction. Because the typical stoichiometry of pyrochlore is $A_2B_2O_7$, 1/8 of the normal anion sites in fluorite are vacant and the oxygens are slightly displaced relative to their nominal positions in stoichiometric fluorite (AO_2). Two types of models have been proposed for the oxygen array. [24] In one, the oxygens form nearly perfect octahedra around the higher valence (B) cation and distorted "cubes" around the much larger, A cations. In a second model, the oxygens are assumed to form nearly perfect cubes around the A cations and distorted octahedra, or rather "perfect" cubes with two vacant corners across the body diagonal. (The structure in Figure 7(c) is represented without anion relaxation to emphasize the structural relationship with the fluorite and perovskite phases.)

Adoption of the pyrochlore structure by an ABO_3 compound such as PZT would introduce an additional 1/8 of oxygen vacancies, for which there is no model available. Some insight, however, may be gained from the ordering reflections noted in Figure 2(c). Calculations by Kwok and Desu [17] suggested that the (111) peak

should be the strongest ordering reflection, which differentiates pyrochlore from fluorite, but this reflection was not observed in the present work. [§] Intensity calculations for both SAD and XRD patterns were undertaken based on the two structural models described above. The first model assumed perfect BO_6 octahedra and oxygen vacancies at the 8b anion sites, i.e. those which are coordinated by four A^{2+}. This is based on the structures of the $PbOsO_3$ and $PbSnO_3$ pyrochlores, which have previously been solved. [25,26] The second model assumed perfect BO_8 cubic cation sites and oxygen vacancies distributed randomly on the 8a, 8b, and 48f sites. [24] (Other vacancy distributions were considered for this model but they had little effect on the estimated intensities.)

Results of the structural calculations are shown in Table 2. It is immediately evident that the intensity of the ordering reflections is strongly influenced by the B-site coordination model and the choice of diffraction technique. The (111) SAD reflection is indeed the strongest reflection for the second model, in agreement with Kwok and Desu, but is essentially absent in the first model in which (331) is the strongest ordering reflection, and (511) the second in relative intensity. That is exactly the case for the experimental observations, suggesting that the first model is better suited to the ordering observed. The model is also consistent with recent FTIR and EXAFS studies on PZT by Lakeman et al. [15] and Sengupta et al., [27] both revealing octahedral coordination of Zr^{4+} and Ti^{4+} in the amorphous material during hydrolysis and partial pyrolysis. The first study also showed that strong IR absorption from BO_6 octahedra persist in PZT films following hydrolysis and pyrolysis, through crystallization of a metastable fluorite phase, and after complete transformation to perovskite.

---

§ The (111) fluorite peak in Figure 2(c) corresponds to the (222) plane of pyrochlore owing to the doubling of the unit cell resulting from ordering.

Notwithstanding the positive identification of the ordering reflections in Figure 2(c) as consistent with pyrochlore, one should note that the relative intensities of these peaks are much lower than those expected for a fully developed structure (see Table 2). One possible scenario is that partial ordering develops uniformly throughout the fluorite phase, or alternatively that a minor fraction of local pyrochlore domains form within the parent fluorite. For example, Haile et al. [28] noted that the incorporation of Zr^{4+} into a $Y_2Ti_2O_7$ pyrochlore promoted intermixing of the A and B-cation sites, leading to a partially ordered structure. Conversely, van Dijk et al. [29] observed antiphase boundaries in $Gd_2Zr_2O_7$, another material which can be prepared with the fluorite or pyrochlore structure, [30] and showed that regions with largely dissimilar degrees of order can develop within the same crystal. Distincton between these scenarios, however, was not possible in the present case on the basis of the information and models available. It is clear, however, that a bulk pyrochlore phase never forms, suggesting that the observed ordering may be a pre-transition phenomenon to the nucleation of perovskite from fluorite.

(3) Compositional Effects on Phase Selection

In spite of the technological importance of PZT, a review of the phase diagram literature reveals that the thermodynamic information on the PbO-ZrO_2-TiO_2 system is rather limited and inadequate for a rigorous, quantitative discussion of the present findings. Conversely, the results of this and other studies on metastable phase selection during the synthesis of PZT do shed further light on the thermodynamics of the system, as discussed below.

It is generally accepted that there is a continuous solid solution field between $PbTiO_3$ and $PbZrO_3$ at high temperatures, wherein the equilibrium structure is the cubic perovskite phase. Quasibinary sections have been proposed for the high [20] and

low [31,32] temperature equilibria, and these are represented in Figure 8(b). The low temperature transformations involve both changes in structure and ferroelectric behavior, presenting substantial challenges to their thermodynamic description. Fortunately, these transformations typically take place below the temperature range wherein crystallization is observed and, thus, one may assume as a first approximation that cubic perovskite is the only competitive *equilibrium* form of PZT for the present experiments. Based on the prior discussion on the nature of the pyrochlore-like ordering, one may further assume that fluorite is also the only relevant metastable phase competing with perovskite along the PTO-PZO quasibinary. The tetragonal ZrO_2 structure is reported to supersede the cubic form with increasing solute content along the ZrO_2-TiO_2 binary, [33,34] and might become competitive with decreasing PbO content, but no evidence of tetragonality was detected in any of the fluorite phases found in the present study. Hence, for simplicity, the discussion is limited to the competition among fluorite, cubic perovskite, and the equilibrium phase assemblages resulting from partitioning, Figure 1(a).

It has been proposed that an upper bound to the stability of a binary solid solution phase when solute partitioning is kinetically constrained is given by the T_0 curve for the solid-liquid transformation.[9] By extension, the metastable single phase fields in a ternary system are bound by the corresponding T_0 surfaces which trace T_0 curves on the isopleths as illustrated in Figure 8. For the case of the stoichiometric ($\chi = 0$) PZT plane, Figure 8(b), the perovskite phase is stable for all temperatures below the $T_0^{L/P}$ trace, whereas the fluorite phase is thermodynamically feasible below $T_0^{L/F}$, but always less stable than perovskite. The $T_0^{L/P}$ curve can be precisely fixed at the PTO end (~1285°C) since this compound melts congruently, but one can only estimate its position on the PZO end, which melts peritectically. Examination of the shape of the PZO liquidus on the ZrO_2-PbO

binary [20] reveals that the hypothetical, congruent melting point of PZO is likely to be well above the peritectic temperature of 1570°C, perhaps as high as ~2000°C. This suggests that the $T_0^{L/P}$ curve rises rather rapidly with ZrO_2 content, as depicted in Figure 8(b), which is consistent with the trend in liquidus and solidus temperatures near PTO.

The position of the $T_0^{L/F}$ curve on the PZT isopleth is more difficult to ascertain. A tentative estimate, depicted in Figure 8(b), was based on the following considerations. The equilibrium solubility limits for TiO_2 in tetragonal and monoclinic ZrO_2 are reported to be substantial, [33] whereas those of PbO are probably much smaller. [20] This suggests that the equilibrium ZrO_2-based fields do not penetrate much into the ternary, as indicated in Figure 1(a). In contrast, the ternary liquidus is apparently dominated by the fluorite region [20] which extends from the pure ZrO_2 corner to ~$Zr_{0.03}Pb_{0.97}O_{1.03}$, ~ $Zr_{0.05}Ti_{0.45}Pb_{0.5}O_{1.5}$, and ~$Zr_{0.45}Ti_{0.55}O_2$. (The latter does not really correspond to fluorite but rather to the tetragonal solution liquidus in the ZrO_2-TiO_2 binary, [33] although this distinction is ignored in Ref. [20].) Available lattice stability functions [35] give a melting point of ~87 K for the fluorite form of pure TiO_2, and that for fluorite-PbO is likely to be even lower. Coupled with an analysis of the binary diagram features this suggests that the traces of the $T_0^{L/F}$ surface drop more or less continuously along the ZrO_2-TiO_2 and ZrO_2-PbO sides of the ternary in Figure 1. It is known, however, that $PbTiO_3$ may be synthesized as a single phase fluorite at temperatures up to at least ~690 K [16], suggesting that the trace of the $T_0^{L/F}$ surface along the TiO_2-PbO binary rises from both ends and has a maximum at some point in the middle. The $T_0^{L/F}$ surface is thus shaped as a "dome" section with a maximum on the ZrO_2 corner, which would form a trace on the PZT isopleth as depicted in Figure 8(b). The rising trend with increasing ZrO_2 content is suggested by the evident stabilization of fluorite with increasing ϕ in Figure 1(b).

Traces of the $T_0^{L/P}$ and $T_0^{L/F}$ surfaces for the $\phi = 0$, 0.33 and 1 isopleths deduced from the known phase equilibria and the results in Figure 1 are plotted in Figure 8(a). The drop in $T_0^{L/P}$ reflects the marked effect of PbO excess or deficiency on the stability of perovskite. The report of a finite homogeneity range on the PbO-lean side, [19] but not for $\chi > 0$, suggests that $T_0^{L/P}$ may drop more rapidly on the PbO-rich side. One may infer from Figure 1(b), however, that the metastable homogeneity range could shift toward higher PbO contents with increasing ZrO_2. The stability of fluorite is less sensitive to deviations from stoichiometry at a constant ϕ, and is expected to increase with ZrO_2 and PbO from the results in Figure 1(b) and the shape of the $T_0^{L/F}$ surface proposed above.

The T_0 curves in Figures 8(a) and (b) suggest some interesting scenarios of phase sequencing relevant to the synthesis of PZTs. On the stoichiometric isopleth, it is clear that if crystallization takes place above the $T_0^{L/F}$ curve one could suppress fluorite formation and the potentially undesirable grain growth effects in the subsequent transformation to perovskite. [16] For this to occur, however, it is necessary to access the region where only perovskite is stable while bypassing nucleation of fluorite during heating, e.g. by rapid thermal annealing. Efforts in this direction have been undertaken by other investigators [36] with no apparent success for the $\phi \approx 1$ PZT composition. Lakeman et al. [15] noted the incipient formation of "ordered" regions within an amorphous PZT matrix prior to the completion of pyrolysis under conditions which eventually led to the crystallization of fluorite. These findings suggest that fluorite nucleation may not be easily suppressible in PZT, even at high heating rates. Conversely, Figure 8(b) also indicates that the probability of bypassing fluorite should increase as $\phi \rightarrow 0$, in agreement with the observations in Figure 1, although one cannot conclusively show at this point that samples containing only perovskite did not go through an intermediate fluorite stage.

The stability of fluorite relative to perovskite should increase with PbO excess or deficiency, as reflected in Figure 8(a), particularly for $\phi > 1$ and $\chi < 0$. Note in this figure that the metastable homogeneity range of fluorite extends beyond that of perovskite, i.e. there are compositions for which metastable fluorite may form but it cannot be transformed to perovskite without partitioning. It is also evident in this figure that the apparent promotion of crystallization by PbO noted in Figure 1 cannot be ascribed to an increased driving force since $T_0^{L/F}$ decreases with addition of excess PbO. The same effect, however, may arise from an increase in atomic mobility within the amorphous phase associated with the addition of PbO. EXAFS studies on amorphous PTO and PZT [27] revealed a network structure consisting of (Ti,Zr)-O-(Ti,Zr) chains, with PbO in random sites within the networks. In essence, PbO appears to behave as a network modifier, with excess PbO increasing the number of unbridged oxygens. This should give rise to a less rigid network which can more easily undergo the rearrangement of ions necessary for crystallization. The opposite is indeed observed when the PbO content is reduced. The $\phi = 1$, $\chi = -0.1$ powder required longer times to initate crystallization than the stoichiometric $\chi = 0$ composition for the same Zr/Ti ratio, even though the former is expected to have a larger driving force for fluorite formation as depicted in Figure 8(a). An additional consequence of this additional driving force is a diminishing potential of partitioning of the metastable fluorite into the equilibrium phases. Indeed, complete partitioning for the $\chi = -0.2$ compositions was not observed even after 1000°C/5min treatments.

(4) Off-stoichiometric Perovskites

The nature of perovskites with extended solubility is of interest owing to the potential effect of the associated defects on their ferroelectric properties. Considerations of the compatibility of the small B^{4+} cations with the 12-fold

coordinated A sites suggest that PbO deficiency is more likely to lead to A-site vacancies than to substitution of Ti^{4+} or Zr^{4+} for Pb^{2+}. This is consistent with observations by other authors on the (Pb,La)TiO_3 system (PLZT), wherein La^{3+} substitutes for Pb^{2+} on the A-site, resulting in an A: B cation ratio of less then one. A-site vacancies were found to be the chief mechanism to accomodate this deviation from the stoichiometric A:B ratio within PLZT. [37]

A more significant issue is whether perovskites synthesized on the hyperstoichiometric side ($\chi > 0$) actually contain excess PbO in solution or are an artifact of PbO losses during the synthesis. Figures 5 and 6 show single phase perovskites with nominal compositions of $\chi = 0.1$ with no apparent sign of fluorite and clear evidence of PbO precipitation during partitioning, indicating that there is indeed excess PbO in solution. Moreover, TGA experiments revealed no significant weight loss under the synthesis conditions of Figure 1, even for pure PbO specimens. For example, only a 0.5% weight loss was measured when ~44 mg of PbO powder were heated at 10°C/min to 800°C and held for 1h in a flow of O_2.

V. CONCLUSIONS

The crystallization behavior of alkoxide-derived amorphous oxides within the PbO-TiO_2-ZrO_2 system was found to depend strongly on both chemical composition and heat treatment temperature. Changes in crystallization temperatures suggest that PbO acts as a modifier within the amorphous network, leading to fewer M-O-M bonds in PbO-excess compositions, which is kinetically more favorable for crystallization.

Single phase perovskites with extended solubility were synthesized, often via a transitional metastable fluorite structure which appears to have a slight degree of pyrochlore-like cation order. The tendency to fluorite formation and its relative stability were enhanced with increasing ZrO_2 concentration, as was the ability to

extend the solubility of PbO into the resulting perovskite. The results suggest that direct crystallization of perovskite from the amorphous precursor, i.e. without fluorite formation, may be more likely near PTO than for PZT.

ACKNOWLEDGEMENTS.

This work was made possible through the support of the Air Force Office of Scientific Research under Grant F49620-93-1-0358DEF and through partial support by NEDO. Support for C.G. Levi was provided under grant DMR/MRL-9123048 from the National Science Foundation. The authors would like to thank Prof. J.S. Speck and Dr. C.D.E. Lakeman for useful discussions, and Mr. D. Stave for technical assistance in the laboratory.

REFERENCES

1. K.D. Budd, S.K. Dey, and D.A. Payne, "Sol-Gel Processing of $PbTiO_3$, $PbZrO_3$, PZT, and PLZT Thin Films", *Br. Ceram. Proc.*, **36** 107-21 (1985).
2. J.B. Blum and S.R. Gurkovich, "Sol-Gel derived $PbTiO_3$," J. Mater. Sci, 20, 4479 (1985).
3. B.A. Tuttle, J.A. Voigt, D.C. Goodnow, D.L. Lamppa, T.J. Headley, M.O. Eatough, G. Zender, R.D. Nasby, and S.M. Rodgers, "Highly Oriented, Chemically Prepared $Pb(Zr,Ti)O_3$ Thin Films", J. Am. Ceram. Soc., 76 [6] 1537-44 (1993).
4. C.D.E. Lakeman and D.A. Payne, "Sol-gel processing of electrical and magnetic ceramics",Mater. Chem. Phys., **38**, 305-24 (1994).
5. F.F. Lange, *Science* **273**, 903 (1996).
6. G. Yi, Z. Wu, and M. Sayer, "Preparation of $Pb(Zr,Ti)O_3$ Thin Films by Sol-Gel Processing: Electrical, Optical, and electro-optic Properties", *J. Appl. Phys.*, **75** [5] 2717-24 (1988).
7. R.W. Vest and W. Zhu, "Films of 60/40 PZT by the MOD Process for Memory Applications", *Ferroelectrics*, 119 61-75 (1991).
8. F.F. Lange, in Chemical Processing of Advanced Materials, (ed. L.L. Hench and J.K. West) p. 611, Wiley, NY (1992).
9. C.G. Levi, "Metastability and Microstructure Evolution in the Synthesis of Inorganics from Precursors," submitted to Acta Materialia (1996).
10. M.L. Balmer, F.F. Lange, and C.G. Levi, "Metastable Phase Selection and Partitioning in ZrO_2-MgO Processed from Liquid Precursors", *J. Am. Ceram. Soc.*, **75** [4] 946-52 (1992).

11. M.L. Balmer, F.F. Lange and C.G. Levi, *J. Am. Ceram. Soc.* **77**, 2069 (1994).

12. P.K. Narwankar, F.F. Lange, and C.G. Levi, to appear in J. Am. Ceram. Soc. Festschrift Issue to honor Arthur Heuer's 60th birthday (1996).

13. V. Jayaram, M. DeGraef, and C.G. Levi, "Metastable Extension of the Fluorite Phase Field in Y_2O_3-ZrO_2 and its Effect on Grain Growth", *Acta Metall. Mater.*, **42** [6] 1829-45 (1994).

14. A.P. Wilkinson, J.S. Speck, A.K. Cheetham, S. Natarajan, and J.M. Thomas, "In Situ X-ray Diffraction Study of Crystallization Kinetics in $PbZr_{1-x}TiO_3$ (PZT, x=0.0, 0.55, 1.0)", *Chem. Mater.*, **6** 750-4 (1994).

15. C.D.E. Lakeman, Z. Xu, and D.A. Payne, "On the Evolution of Structure and Composition in Sol-Gel Derived Lead Zirconium Titanate Thin Layers", *J. Mater. Res.*, **10** [8] 2042-51 (1995).

16. A. Seifert, F.F. Lange, and J.S. Speck, "Epitaxial Growth of PbTiO3 Thin Films on (001) SrTiO3 from Solution Precursors", *J. Mater. Res.*, **10** [3] 680-691 (1995).

17. C.K. Kwok and S.B. Desu, "Pyrochlore to Perovskite Phase Transformation in Sol-Gel Derived Lead-Zirconium-Titanate Thin Films", Appl. Phys. Lett., **60** [12] 1430-2 (1992).

18. A.D. Polli and F.F. Lange, "Pyrolysis of $Pb(Zr_{0.5}Ti_{0.5})O_3$ Precursors: Avoiding Lead Partitioning", J. Amer.Ceram. Soc. 78 [12] 3401-4 (1995).

19. R.L. Holman and R.M. Fulrath, "Intrinsic Nonstoichiometry in the Lead Zirconate-Lead Titanate System Determined by Knudsen Effusion", J. Appl. Phys., **44** [12] 5227-36 (1973).

20. S. Fushimi and T. Ikeda, *J. Am. Ceram. Soc.* **50** [3] 131, 132 (1967).

21. M.A. Eisa, M.F. Abadir, and A.M. Gadalla, *Trans. J. Br. Ceram. Soc.* **79**[4] 100-4 (1980).

22. A.H. Webster, R.C. MacDonald, and W. S. Bowman, *J. Can. Ceram. Soc.* **34**, 99 (1965).

23. J.M. Longo, P.M. Raccah and J.B. Goodenough, "$Pb_2M_2O_{7-x}$ (M = Ru, Ir, Re) - Preparation and Properties of Oxygen Deficient Pyrochlores," *Mat. Res. Bull.* 4, 191-202 (1969).

24. M.A. Subramanian, G. Aravamudan, and G.V. Subba Rao, "Oxide Pyrochlores- a Review", Prog. Solid State Chem., **15** [2] 55-143 (1983).

25. J.P. Badaud and J. Omaly, "Preparation and Properties of a New Pyrochlore $Pb_2Os_2O_3$", C.R. Acad. Sc. Paris, Ser. C, **274** 178-80 (1972).

26. B.I. Morgenstern and M.A. Michel, "A Compound of Pyrochlore Type: $Pb_2Sn_2O_3$, xH_2O", Ann. Chim., **1971** 109-24 (1971).

27. S.S. Sengupta, L.Ma, D.L. Adler, and D.A. Payne, "Extended X-ray Absortion Fine Structure Determination of Local Structure in Sol-Gel Derived Lead Titanate, Lead Zirconate, and Lead Zirconium Titanate", J. Mater. Res., **10** [6] 1345-8 (1995).

28. S.M. Haile, B.J. Wuensch, and E. Prince in Neutron Scattering for Materials Science, Proc. Symp. Vol. 166, Boston, MA, 1989, eds. S.M. Shapiro, S.C. Moss, and J.D. Jorgensen (Mater. Res. Soc., Pittsburgh, PA, 1990) pp.81-6.

29. M.P. van Dijk, F.C. Mijlhoff, and A.J. Burggraf, "Pyrochlore Microdomain Formation in Fluorite Oxides", *J. Solid State Chem.*, **62** 377-85 (1986).

30. T. Uehra, K. Koto, and F. Kanamaru, "Stability and Antiphase Domain Structure of the Pyrochlore Solid Solution in the ZrO_2-Gd_2O_3 System", *Solid State Ionics*, **23** 137-43 (1987).

31. E. Sawaguchi, *J. Phys. Soc. Japan,* **8**, 615 (1953).

32 O.E. Fesenko, V.G. Smotrakov, and N.G. Leont'ev, *Ferroelectrics* **63** [1-4] 189-96 (1985).

33. A.E. McHale and R.S. Roth, *J. Am. Ceram. Soc.* **66** [2] C18-20 (1983).

34. A.E. McHale and R.S. Roth, *J. Am. Ceram. Soc.* **69** [11] 827-32 (1986).

35. L. Kaufman, "Calculation of Multicomponent Ceramic Phase Diagrams," *Physica B* **150**, 99-114 (1988). 36 E.M. Griswold, L. Weaver, M. Sayer and I.D. Calder, "Phase Transformations in Rapid Thermal Processed Lead Zirconate Titanate," *J. Mater. Res.* **10** [12] 3149-59 (1995).

36. E.M. Griswold, L. Weaver, M. Sayer and I.D. Calder, "Phase Transformations in Rapid Thermal Processed Lead Zirconate Titanate," *J. Mater. Res.* **10** [12] 3149-59 (1995).

37. G. Rossetti, M.A. Rodriguez, A. Navrotsky, L.E. Cross, and R.E. Newnham, "Structure of the Defect Perovkite $[Pb_{0.85}La_{0.10}]TiO_3$ Between 10 and 1023K", J. Appl. Phys., **77** [4] 1683-9 (1995).

Table 1. Lattice Parameters of Metastable Phases.

Zr/Ti	PbO	Perovskite				Fluorite	
ϕ	χ	a	c	c/a	$V_{f.u.}$	a	$V_{f.u.}$
0	-0.2	3.9936(22)	4.0353(47)	1.010	64.4	5.13	67.5
	-0.1	3.9188(27)	4.0778(87)	1.041	62.6	-	-
	0	3.9091(8)	4.1330(17)	1.057	63.2	-	-
	0.1	3.9121(13)	4.1519(36)	1.061	63.5	-	-
0.33	-0.2	3.9675(12)	4.1017(29)	1.034	64.6	5.17	69.1
	-0.1	3.9722(8)	4.1094(15)	1.035	64.8	5.19	69.9
	0	3.9728(11)	4.1261(21)	1.039	65.1	-	-
	0.1	3.9639(14)	4.1498(23)	1.047	65.2	-	-
	0.2	-	-	-	-	5.24	71.9
1	-0.2	4.079	~4.079	~1.0	67.9	5.26	72.8
	-0.1	4.0496(31)	4.0899(37)	1.010	67.1	5.24	71.9
	0	4.0419(26)	4.1051(41)	1.016	67.1	5.25	72.4
	0.1	4.0304(20)	4.1089(31)	1.019	66.7	5.25	72.4

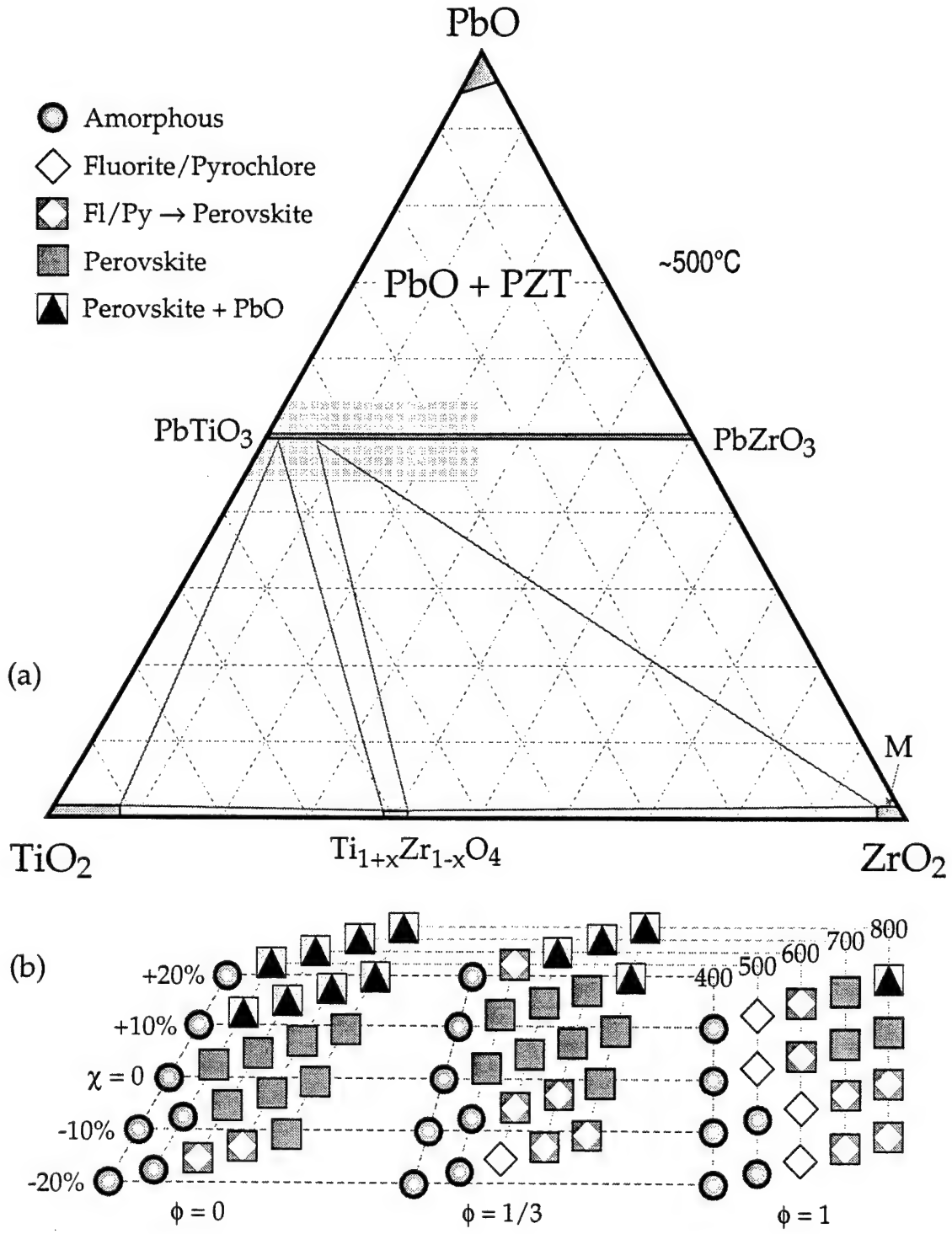

Figure1. Tentative 500°C isothermal section of the PbO-ZrO_2-TiO_2 phase diagram (a) based on references [20], [21], [31], [33], and [34]. The shaded region in (a) represents the composition range investigated. Phase evolution within this region is depicted in (b) as a function of Zr/Ti ratio (ϕ) and PbO excess/deficiency (χ). In all cases the phase(s) depicted are for 5 min treatments after heating rapidly to the temperatures indicated. For any given (ϕ,χ) combination the temperature increases from left to right.

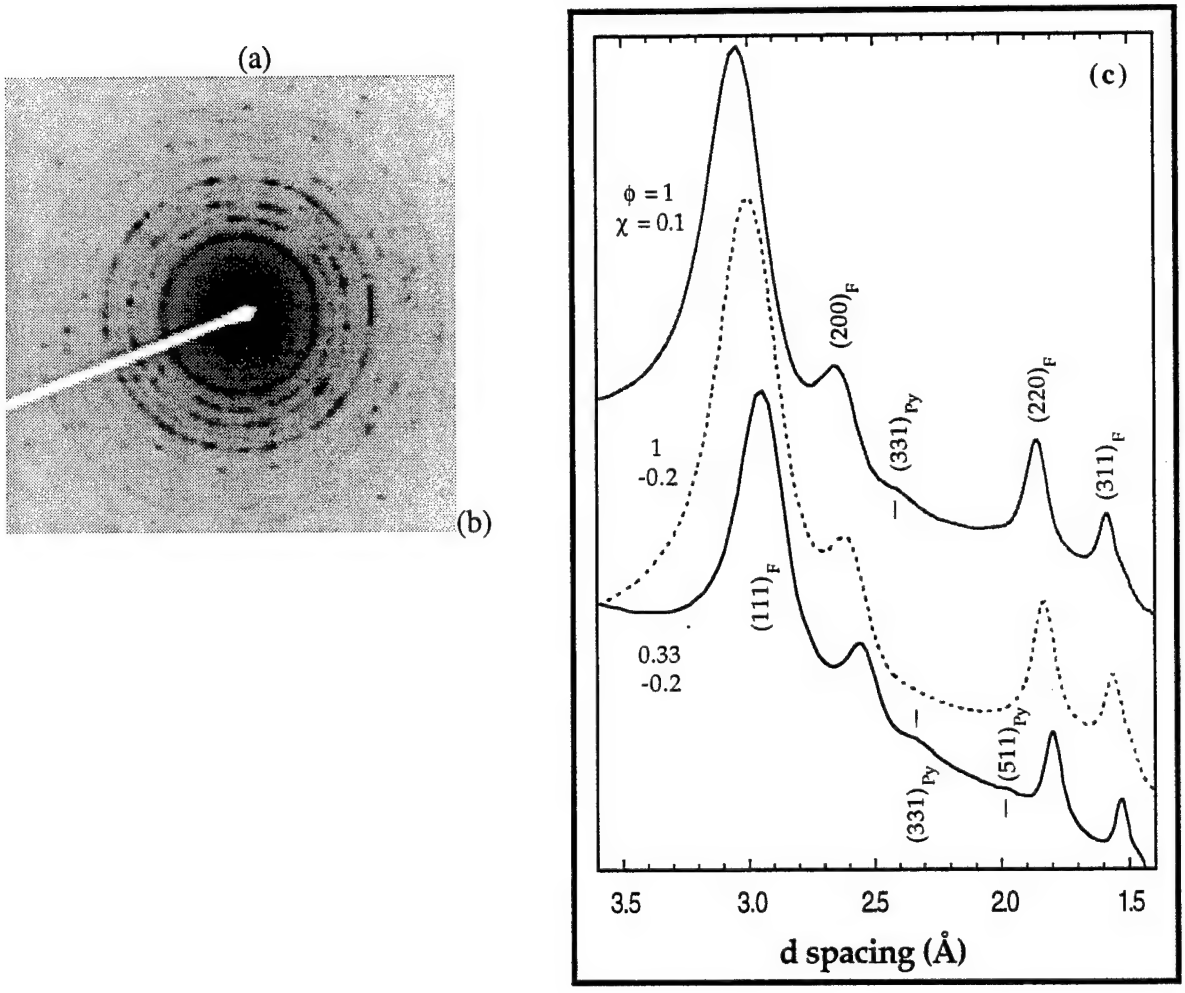

Figure 2. Typical SAD patterns for fluorite (a) and perovskite (b) obtained from particles with composition ϕ=1, χ=0.1 heat treated at 500°C/5min and 600°C/4h, respectively. Rotationally averaged profiles of SAD patterns from χ/ϕ combinations of 0.1/1 (top), -0.2/1 (middle) and -0.2/0.33 (bottom). The weak peaks in the top and bottom curves correspond to the (331) and (511) ordering reflections of pyrochlore, as labeled, which are not detectable in the middle curve.

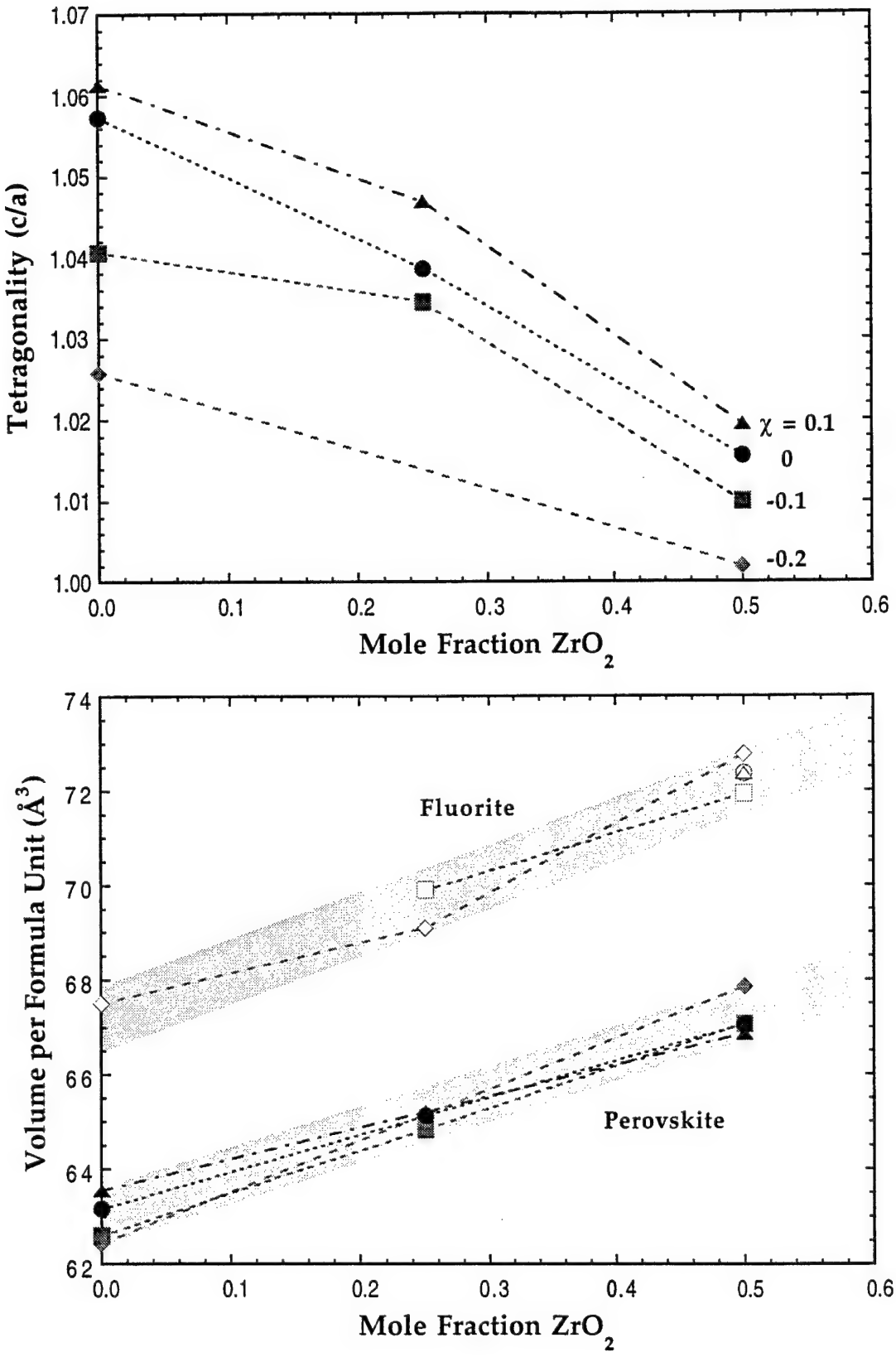

Figure 3. Tetragonality (c/a ratio) of the perovskite phase resulting from precursor pyrolysis as a function of composition (a). (b) depicts the volume per formula unit for the fluorite and perovskite cells as a function of composition.

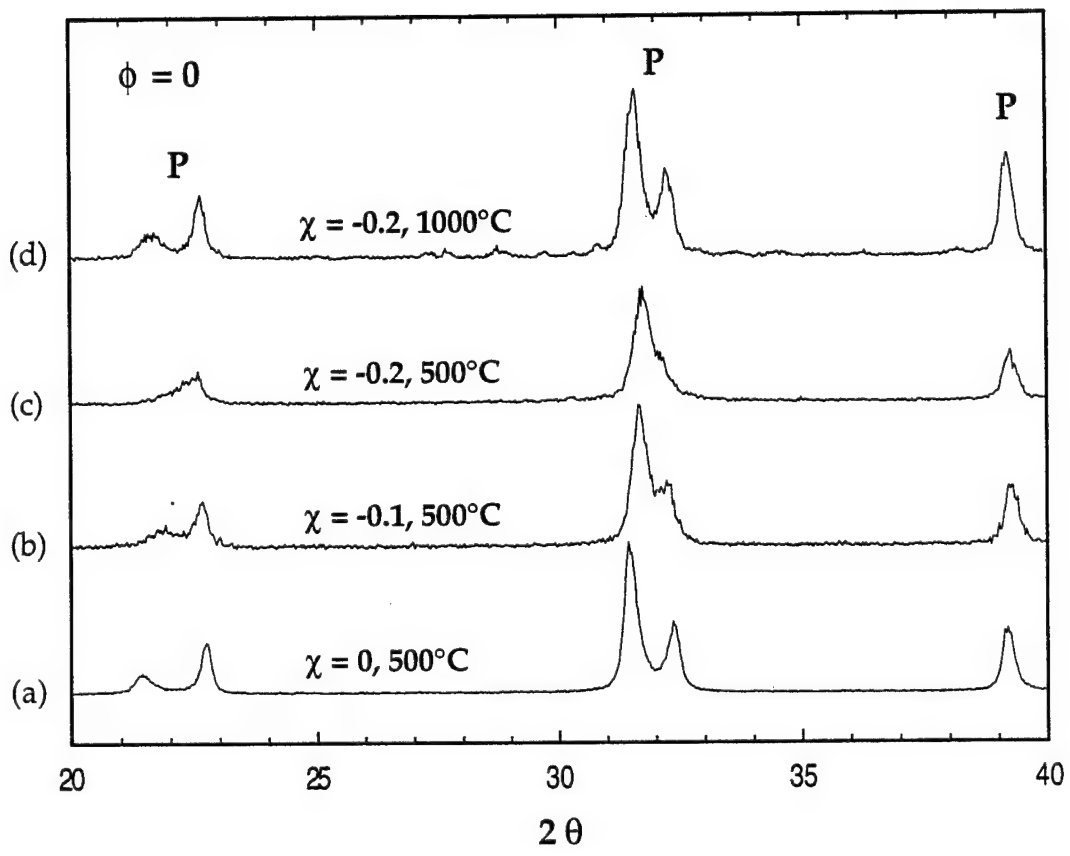

Figure 4. XRD patterns for lead titanate compositions with (a) χ=0, (b) χ =-0.1, and (c) χ =-0.2 heat treated at 500°C, and (d) χ =-0.2 treated at 500°C with a subsequent heating of 1000°C. The times in all cases are 5 min.

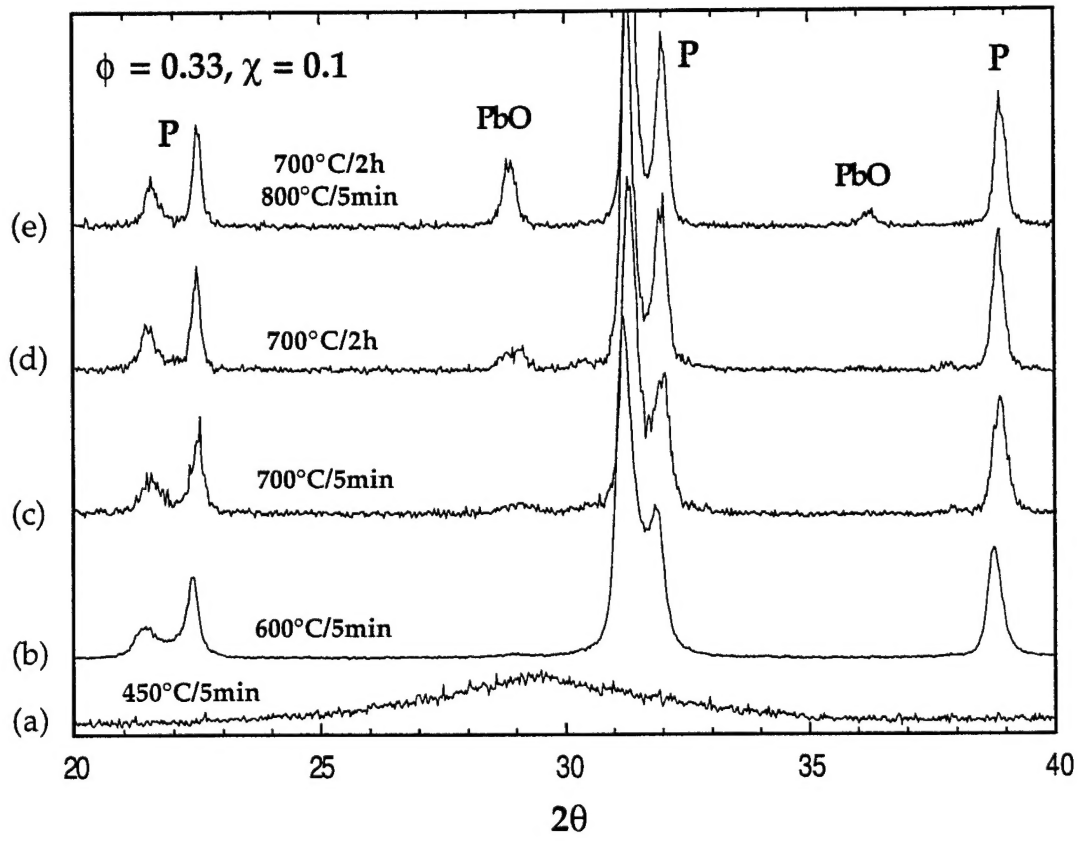

Figure 5. XRD patterns for ϕ=0.33, χ=0.1 material heat treated at (a) 450°C/5min, (b) 600°C/5min, (c) 600°C/5min, (d) 700°C/2h, and (e) 700°C/2h with subsequent heating of 800°C/5min.

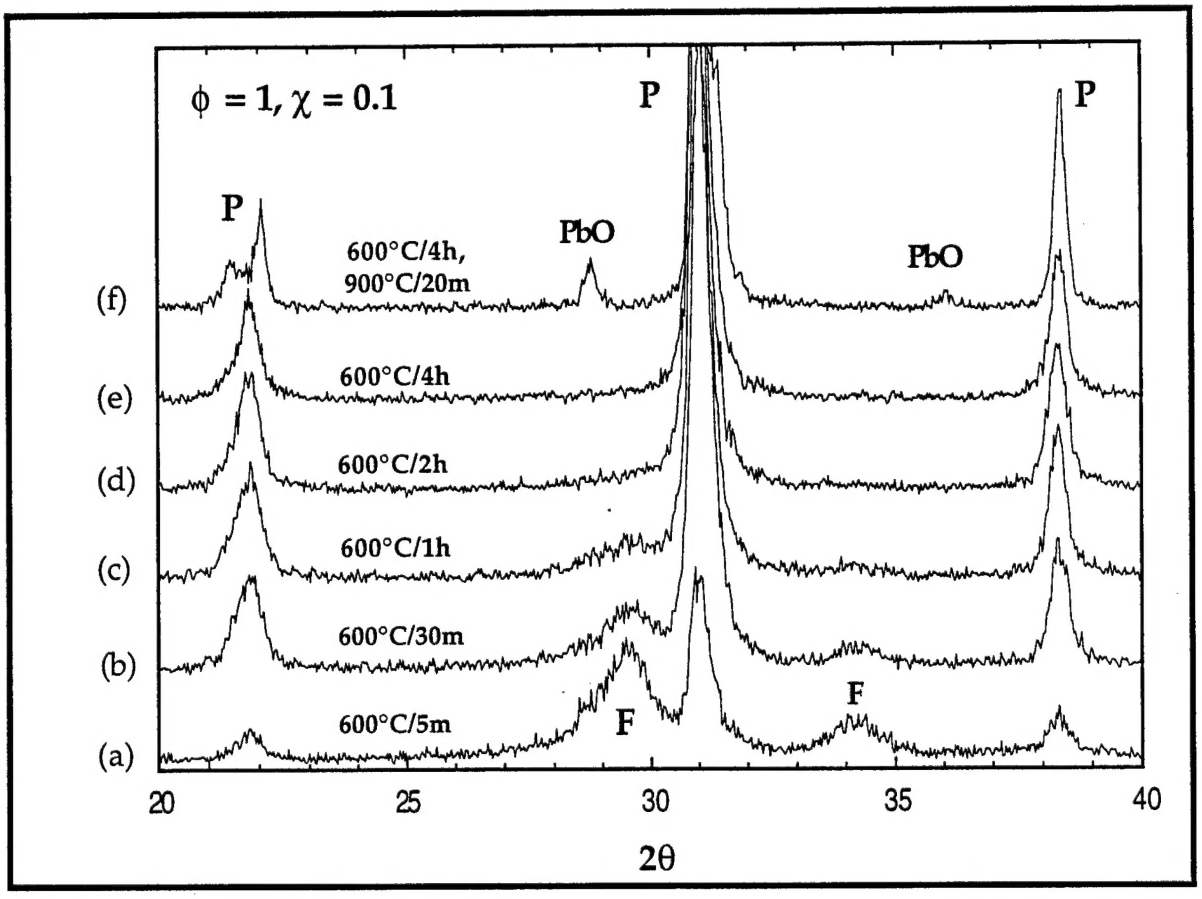

Figure 6. XRD patterns for ϕ=1, χ=0.1 material heat treated at 600°C for (a) 5min, (b) 30min, (c) 1h, (d) 2h, (e) 4h, and (f) 4h with subsequent heating at 900°C/20min.

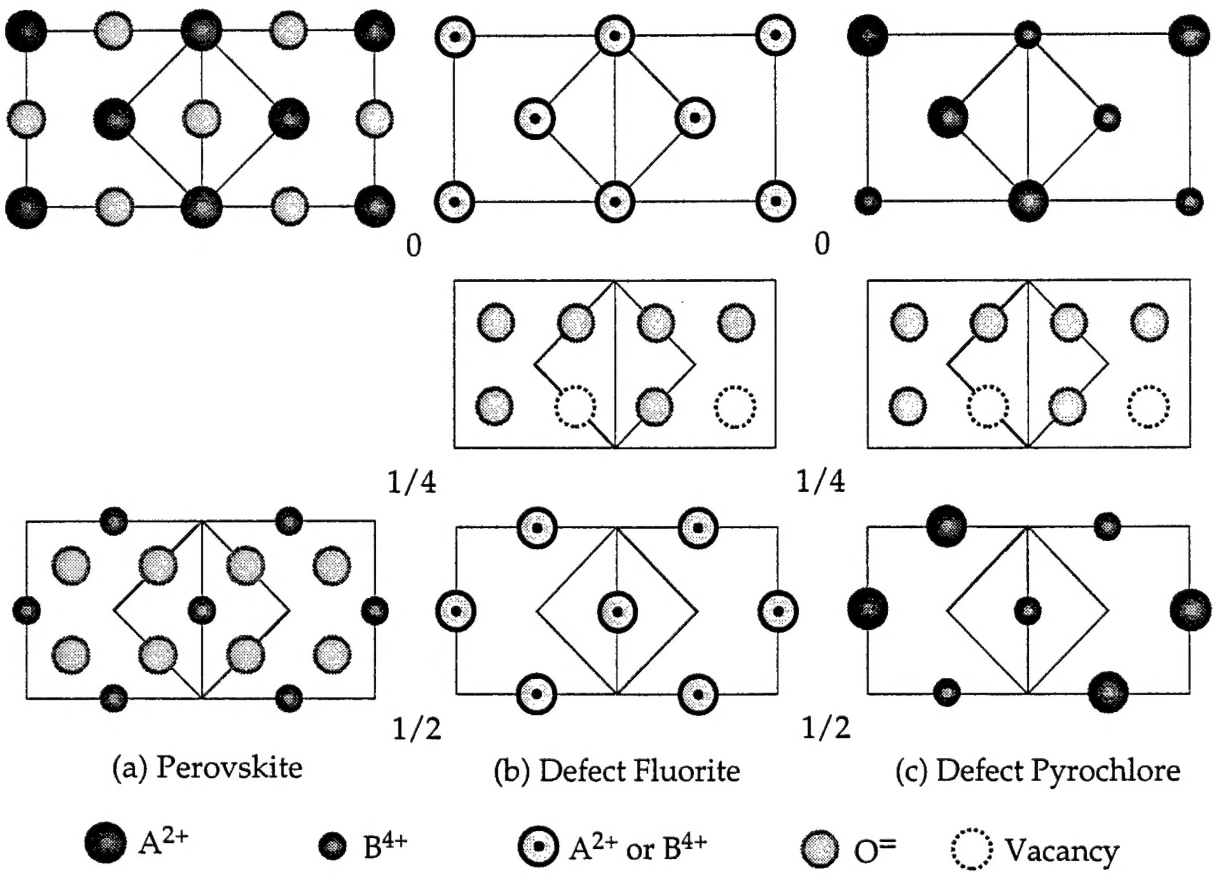

Figure 7. Structural relationships between the (a) perovskite, (b) defect fluorite, and (c) defect pyrochlore structures. The positions of the ions in the defect fluorite and perovskite are presented as they would be in a perfect fluorite structure, without allowing for the relaxation expected from the presence of anion vacancies.

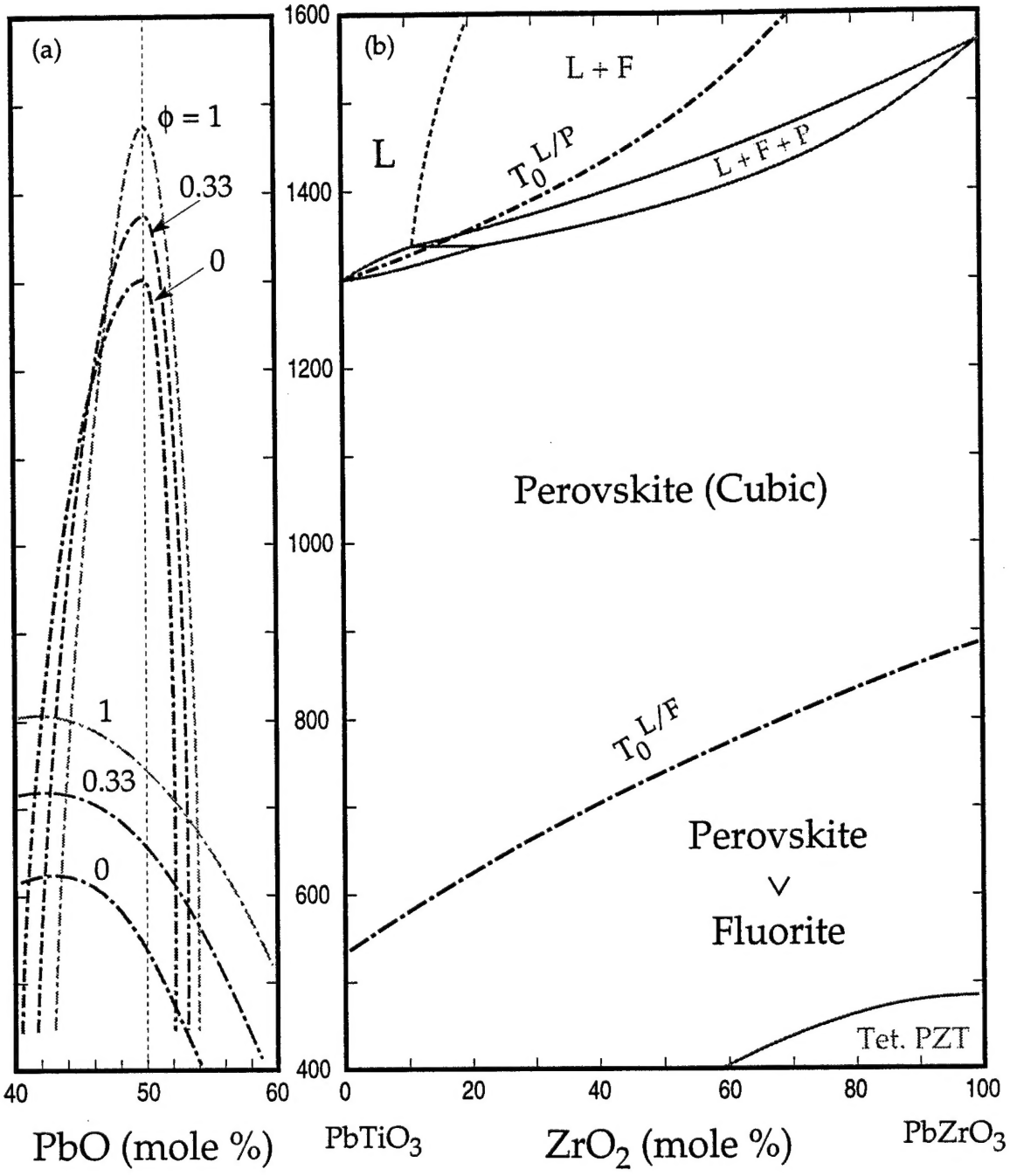

Figure 8. T_0 traces for the cubic perovskite and defect fluorite structures (a) for different ϕ ratios as a function of PbO concentration and (b) for the PTO-PZO quasibinary ($\chi = 0$).